Time-domain and frequency-domain macromodeling: application to package structures

(Article begins on next page)

18 April 2024

Time-Domain and Frequency-Domain Macromodeling: Application to Package Structures

S. Grivet-Talocia, I. S. Stievano, I. A. Maio, F. Canavero

Dipartimento di Elettronica, Politecnico di Torino,
Corso Duca degli Abruzzi 24, 10129, Torino, Italy
{grivet,stievano,maio,canavero}@polito.it

Abstract

This paper applies different macromodeling strategies for the generation of SPICE-ready equivalent circuits of complex multiport package structures. In particular, accuracy comparisons are performed between two techniques capable of processing either time-domain or frequency-domain responses for the derivation of the macromodel. The time-domain tool is an implementation of a Subspace-based State-Space System Identification (4SID) technique specifically designed for the analysis of structures with a large number of ports. The frequency-domain tool is the powerful pole relocation algorithm known as Vector Fitting. The two methods are compared through application to a realistic package example. The passivity of the macromodels is enforced using a powerful technique based on perturbation of associated Hamiltonian matrices.

INTRODUCTION

The high complexity of modern electronic systems require sophisticated modeling tools in order to assess all critical aspects of a design. In particular, Signal Integrity (SI) and ElectroMagnetic Compatibility (EMC) assessments are among the most challenging modeling tasks. Since a system-level full-wave electromagnetic analysis is not feasible, approximate modeling is required. One possibility is to identify suitable structures that can be treated as single blocks interacting with the environment only through well-defined ports, and attempt the derivation of suitable macromodels or equivalent circuits with reduced complexity. The latter are then used in system-level simulations using a standard circuit solver like, e.g., SPICE.

There are several approaches that can be adopted for the generation of macromodels for a given interconnect or package structure. One possibility is to generate a large equivalent circuit from the three-dimensional mesh using a full-wave discretization tool (like, e.g., the PEEC method), and to apply some model order reduction technique to reduce it to a feasible size. Usually Krylov subspace techniques are employed for the model reduction part [1, 2]. A complementary approach is to derive the macromodel from either simulated or measured responses, either in time or in frequency domain. The input/output sampled responses are the raw data required by the macromodeling algorithm. Therefore, the device under modeling is treated as a black-box of which all port responses to some excitation are known. We concentrate on this second approach in this work.

Among the many available macromodeling techniques we focus our attention specifically on two methods, which appear to be well-suited for application to realistic package structures with many ports. The first technique belongs to the class of the so-called Subspace-based State-Space System Identification (4SID) methods [3], of which an implementation specifically tailored for packages has been described in [5], where the main properties of the algorithm are detailed. The core of the method involves processing all transient waveforms of the port responses in order to estimate a set of poles which will be common to all tranfer functions of the macromodel. Once these poles are known, the matrices of residues for the corresponding rational approximation are computed via standard least squares. Synthesis of an equivalent circuit from the rational approximation is a standard and easy task.

The second technique that will be considered is Vector Fitting (VF) [4]. It works entirely in frequency domain by producing an estimate for the dominant poles of the structure using an iterative algorithm that refines at each step this estimate. The convergence properties are very good since typically in very few iterations quite accurate estimates for the poles are reached. Once the poles are known, the same steps of 4SID are followed to generate the equivalent circuit. Therefore, both 4SID and VF produce poles, the first using time-domain responses, and the second using frequency-domain data. The rest of the macromodeling process proceeds following common steps. We remark that the poles estimation is the most critical one, since the poles are the basic ingredients for a good representation of the actual dynamic behavior of the structure under investigation.

Once an accurate macromodel has been generated, it has to be checked for passivity. It is well known that stable but non-passive macromodels may lead to instability when connected to termination networks that are different from those used for the identification of the macromodel itself. We apply a powerful technique based on spectral perturbation of associated Hamiltonian matrices for this task. This technique [7] allows to compensate any passivity violations by an iterative proce-

dure applied to a state-space realization of the macromodel.

The outline of this paper is as follows. A brief description of VF and 4SID algorithms is given in Sections 1 and 2. Application to macromodeling of a 16-pin surface mount package is detailed in Section 3. Finally, some remarks on the passivity enforcement of the macromodels are given in Section 4.

1 VECTOR FITTING

We consider a package structure with an arbitrary number P of ports and characterized by a matrix transfer function $\mathbf{H}(s)$. The objective is the derivation of a rational approximation to the matrix transfer function $\mathbf{H}(s)$, where s is the Laplace variable. This approximation reads, in terms of poles and residues,

$$\mathbf{H}(s) \simeq \mathbf{H}_\infty + \sum_{n=1}^{N} \frac{\mathbf{R}_n}{s - p_n} . \tag{1}$$

Note that the N poles are common to all matrix entries, whereas the direct coupling term and the residues are $P \times P$ matrices.

The standard VF algorithm [4] processes a set of frequency samples of the above transfer matrix and estimates the poles via an iterative scheme. At each iteration a linear least squares system is solved. This is achieved by introducing a scalar weight function

$$\sigma(s) = 1 + \sum_{n=1}^{N} \frac{k_n}{s - q_n} = \frac{\prod_{n=1}^{N}(s - z_n)}{\prod_{n=1}^{N}(s - q_n)} \tag{2}$$

with known (initial) poles $\{q_n\}$ and unknown residues $\{k_n\}$. Let us assume now that the following approximation holds,

$$\sigma(s)\mathbf{H}(s) \simeq \mathbf{M}_\infty + \sum_{n=1}^{N} \frac{\mathbf{M}_n}{s - q_n} . \tag{3}$$

Since the right-hand-side has the same poles $\{q_n\}$ as the weight function, a cancellation between the zeros $\{z_n\}$ of $\sigma(s)$ and the poles $\{p_n\}$ of $\mathbf{H}(s)$ must occur. This condition provides indeed a way to estimate these poles by solving (3) for the unknown residues $\{k_n\}$, computing the zeros $\{z_n\}$ using standard techniques [4], and by enforcing $p_n = z_n$. This procedure, named *pole relocation*, avoids use of ill-conditioned nonlinear least squares algorithms for the direct approximation of (1). The poles relocation is then iterated using the estimated poles as starting poles for each new step. Convergence is usually reached in very few iterations.

When applied to structures with a very large number of ports, the size of the least squares system (3) may grow very large. In fact, all matrix entries at all frequency points must be processed at once. Therefore, in order to avoid excessive memory requirements, we consider only a subset of entries in the transfer matrix to be used for the identification of the poles. After extensive testing on several structures, we conclude that a good criterion for the selection of these elements

is to consider the entries characterized by the largest energy content in the modeling bandwidth. For packages, this corresponds to the inclusion of the direct transmission and reflection coefficients on each pin. If possible, also the largest crosstalk coefficients may be considered. The small couplings are instead not used for the poles estimation.

Once the poles $\{p_n\}$ are known, the residues $\mathbf{R}_n$ and the direct coupling matrix $\mathbf{H}_\infty$ are computed componentwise by solving (1) in least squares sense. Note that only one matrix entry can be processed at the time. Therefore, this step is less demanding than the poles computation even in case of many ports. Synthesis of a SPICE-ready equivalent circuit from this rational approximation may be obtained following a standard procedure, which is not detailed here.

2 SUBSPACE-BASED STATE-SPACE SYSTEM IDENTIFICATION

The class of 4SID methods [3] is aimed at the determination of a state-space representation of the structure under modeling via direct identification of the state matrices. Among these methods, we employ here a particular implementation [5, 10] specifically designed to handle structures with a possibly large number of ports. The raw data to be used for the identification consists of a complete set of transient waveforms of outputs y_k, where k denotes the time index with a suitable sampling time T_s, subject to some combination of input waveforms u_k. Since these sequences are sampled, it is convenient to focus our attention on the discrete-time state-space system

$$\begin{cases} x_{k+1} & = & \widetilde{A}x_k + \widetilde{B}u_k \\ y_k & = & \widetilde{C}x_k + \widetilde{D}u_k \end{cases} \tag{4}$$

where x denotes the set of internal discrete-time states. Only the main steps of the identification algorithm are reported, more details can be found in [5, 10].

First, we rewrite the system (4) as

$$\mathbf{Y} = \mathbf{\Gamma}\mathbf{X} + \mathbf{\Phi}\mathbf{U} , \tag{5}$$

where $\mathbf{U}, \mathbf{Y}, \mathbf{X}$ denote block Hankel matrices of input, output, and state time sequences, respectively. Given some discrete-time sequence z_k, the corresponding block Hankel matrix is constructed using the available samples as $(\mathbf{Z})_{ij} = z_{i+j-1}$. The unknowns in the above expression are both the coefficient matrices $\mathbf{\Gamma}$, $\mathbf{\Phi}$, and the state Hankel matrix $\mathbf{X}$. However, we only need an estimate for the matrix $\mathbf{\Gamma}$, which is the observability matrix of (4) defined as

$$\mathbf{\Gamma} = \begin{bmatrix} \widetilde{C} \\ \widetilde{C}\widetilde{A} \\ \widetilde{C}\widetilde{A}^2 \\ \vdots \end{bmatrix} . \tag{6}$$

This estimate is achieved through a suitable projection of $\mathbf{Y}$ onto some linear space orthogonal to $\mathbf{U}$. This corresponds to
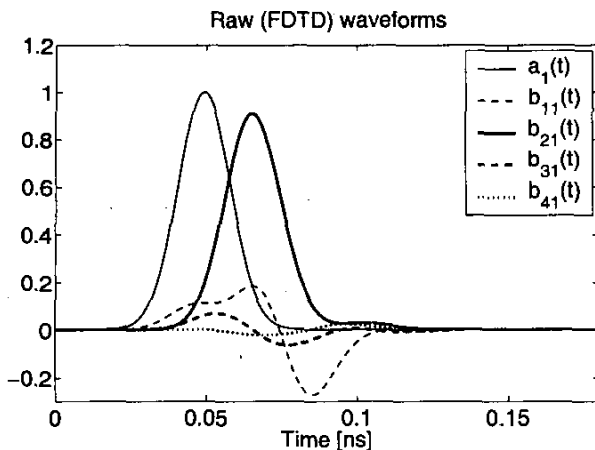
Figure 1: Some of the transient scattering waveforms obtained as output from FDTD modeling a package structure.

Figure 2: Poles estimated from 4SID and VF algorithms for the same package structure.

extracting the dynamic part of the input-output relation, since the result of this projection corresponds to "what is missing" from the input sequences to obtain the output sequences. This projection is performed using a standard RQ factorization combined with a singular value decomposition. Once Γ is known, its shift invariance property is used to estimate the discrete-time state matrix $\tilde{A}$, and consequently the poles of the discrete macromodel. The poles of a continuous-time realization are finally obtained by a discrete-to-continuous transformation.

As for the VF implementation described in Section 1, not all responses are needed for the poles estimation. We consider also for the 4SID implementation a set of dominant resposes, which we use for the estimation of the global poles of the macromodel. In fact, even though the time sequences can be pre-processed and sub-sampled at the Nyquist frequency corresponding to the modeling bandwidth (of course paying particular attention to aliasing problems), the size of the block Hankel matrices in (5) may grow very large in case of a large number of ports. Therefore, only few significant responses are used. The corresponding matrices of residues are estimated componentwise by standard least squares using the complete set of time responses.

3 PACKAGE MACROMODELING

We first apply the two mentioned macromodeling techniques to the characterization of a 16-pin surface mount package structure. The aim is to produce a fully coupled lumped macromodel able to reproduce with high accuracy both time and frequency behavior of the package within an extended band of frequency. Although the package is not designed for such high frequencies, we attempt the construction of a macromodel using a bandwidth of 40GHz. This is intended to stress as much as possible the two algorithms that are in-
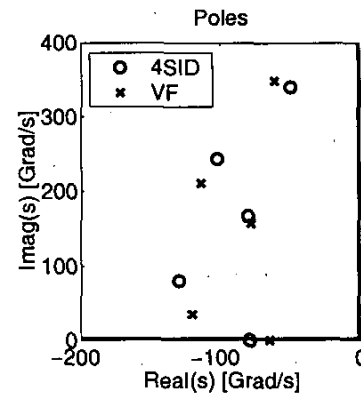
vestigated in this work.

A complete set of input-output responses are obtained through a full-wave modeling tool based on a standard Finite-Difference Time-Domain (FDTD) scheme [6]. Some of these output responses (transient scattering waves) obtained from excitation of a single port (with the other ports terminated into 50 Ω loads) are depicted in Fig. 1. This is the raw dataset to be processed by 4SID algorithm. Frequency-domain scattering parameters are then obtained by applying FFT to the time-domain transient responses, and will be the raw data to be processed by VF algorithm.

Both 4SID and VF lead to a set of poles for the structure, depicted in Fig. 2. Note that the estimates for the most resonant poles are quite close for the two methods. The less resonant poles, which have less influence on the frequency-domain behavior of the macromodel, are somewhat different. This is expected, since the estimation criteria for the two methods are completely different. Nonetheless, the scattering parameters for the 4SID and VF macromodels are extremely accurate, as shown in Fig. 3 for some matrix entries.

As a further validation in time-domain, we have repeated the FDTD simulation by terminating the hot pin and its neighbor into a 10 kΩ/1 pF load, leaving the other ports unchanged, and recording the near and far end voltages excited by a smooth step voltage source. We then performed two SPICE runs using the equivalent circuits generated from 4SID and VF rational approximations. The results are shown in Fig. 4. The transient voltage curves confirm the excellent accuracy of both macromodels. Based on this example, our conclusions are that both the presented macromodeling techniques based on 4SID and VF lead to very accurate macromodels. The choice of a specific technique to be adopted for the macromodel generation depends on the format of the available raw data.
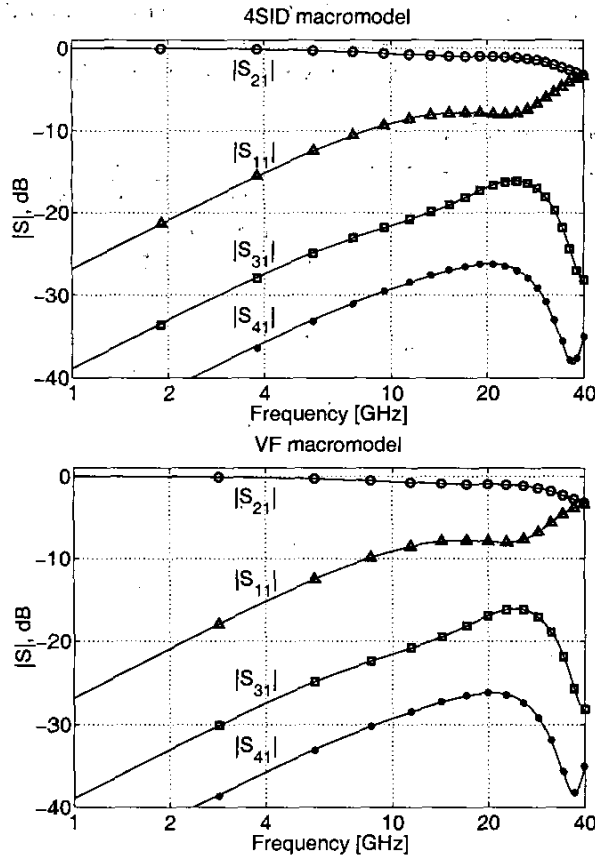
572

Figure 3: Some of the scattering parameters for the macromodels (markers) obtained with 4SID (top) and VF (bottom) compared to the raw data (solid lines).

4 PASSIVITY

The macromodels generated by either VF or 4SID algorithms are not guaranteed to be passive. Therefore, some test for passivity must be applied and, in case of passivity violations, some compensation must be performed. Due to the excellent accuracy of the macromodeling tools that are used in this work, any passivity violation is expected to be small. Therefore, some a posteriori correction algorithm can be used without difficulty.

Several tests for passivity are available in the literature. One possibility is to perform a frequency sweep of the transfer matrix and to check the passivity at each frequency. This technique requires accurate frequency sampling, which is critical. A more reliable test is based on the determination of the eigenvalues of some associated Hamiltonian matrices. The construction of the latter requires a state-space realization of the macromodel, which can be easily constructed following, e.g., the procedure detailed in [8]. We denote the state matrices as $\{A, B, C, D\}$. The form of the Hamiltonian matrix depends on the multiport representation of the
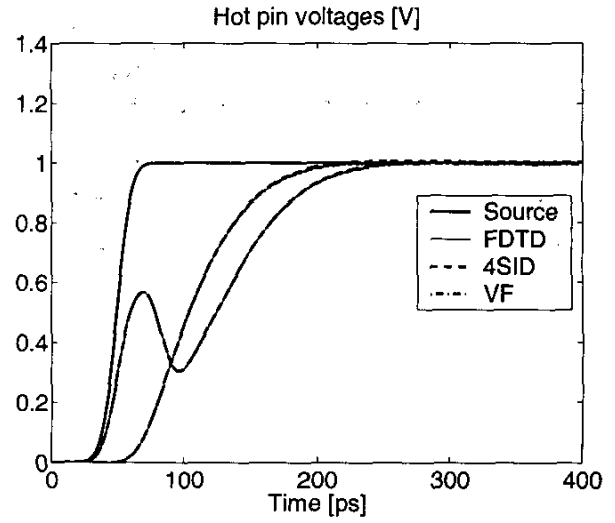

Figure 4: Transient voltages at near and far end of a hot pin of the package loaded at the far end with 10 kΩ/1 pF loads. The waveforms obtained from SPICE simulations of the macromodels are compared to those resulting from a full-wave FDTD simulation.

macromodel. In case of scattering representations we have

$$M = \begin{pmatrix} A - BR^{-1}D^T C & BR^{-1}B^T \\ C^T S^{-1}C & -A^T + C^T D R^{-1}B^T \end{pmatrix},$$
(7)

where $R = (D^T D - I)$ and $S = (DD^T - I)$. Instead, in case of impedance, admittance, or hybrid representations, we have

$$N = \begin{pmatrix} A + BQ^{-1}C & BQ^{-1}B^T \\ -C^T Q^{-1}C & -A^T - C^T Q^{-1}B^T \end{pmatrix},$$
(8)

where $Q = -(D + D^T)$. The macromodel is guaranteed to be passive if the above matrices have no purely imaginary eigenvalues [9].

If some imaginary eigenvalues are present, then the macromodel might be non-passive. In such case, we apply the compensation algorithm detailed in [7]. This algorithm is based on the iterative displacement of the imaginary eigenvalues through application of first-order perturbation theory to the Hamiltonian matrix. See [7] for a detailed description.

We illustrate the effectiveness of this algorithm through an example, consisting of a multilayer PCB with several power and ground planes crossed by 9 via interconnects throughout its cross-section. The resulting structure has therefore $p = 18$ ports. The structure has been meshed and analyzed with a full-wave electromagnetic solver based on the Finite-Difference Time-Domain (FDTD) method. All ports are defined using a 50Ω reference load. The raw dataset obtained by FDTD is a set of 18 × 18 transient scattering responses due to Gaussian pulse excitation having a 6 GHz frequency
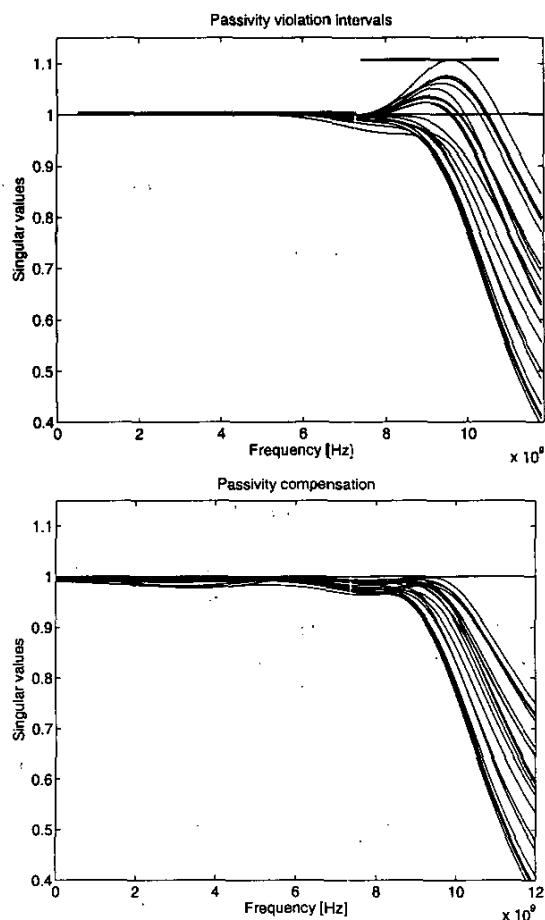
Figure 5: Passivity compensation for a macromodel of a multiple via structure. The singular values are plotted versus frequency for the non-passive macromodel (top panel) and for the passive macromodel (bottom panel).

bandwidth. This set of responses has been processed by VF algorithm in order to derive a rational macromodel. An excellent approximation was obtained using only $n_p = 6$ poles. This approximation was then converted to a full state-space realization with order $n = 18 \times 6 = 108$. Although very accurate, the resulting state-space realization is not passive, as depicted in the top panel of Fig. 5 The figure reports the singular values of the scattering matrix plotted versus frequency. Note that the passivity violation within the modeling bandwidth is very small, while the violation is more significant at higher frequencies. The bottom panel of Fig. 5 shows the singular values distribution of the passive macromodel. All singular values are now uniformly bounded by one as required by the passivity condition.

5 ACKNOWLEDGEMENTS

This work is supported in part by the Italian Ministry of University (MIUR) under a Program for the Development of Re-

REFERENCES

[1] I. Erdin, M. Nakhla, R. Achar, "Circuit Analysis of Electromagnetic Radiation and Field Coupling Effects for Networks with Embedded Full-Wave Modules", *IEEE Trans. Electromaget. Compat.*, **42**, 2000, 449–460.

[2] A. Odabasioglu, M. Celik, L. T. Pileggi, "PRIMA: passive reduced-order interconnect macromodeling algorithm," *IEEE Trans. Computer-Aided Design of Int. Circ. and Sys.*, **17**, 1998, 645–654.

[3] M. Viberg, "Subspace-based methods for the identification of linear time-invariant systems," *Automatica*, Vol. 31, No. 12, pp. 1835–1851, 1995.

[4] B. Gustavsen, A. Semlyen, "Rational approximation of frequency responses by vector fitting", *IEEE Trans. Power Delivery*, Vol. 14, July 1999, pp. 1052–1061.

[5] S. Grivet-Talocia, F. Canavero, I. Maio, and I. Stievano, "Reduced-order macromodeling of complex multiport interconnects," in *URSI General Assembly, Maastricht, Belgium*, August 19–23, 2002.

[6] A. Taflove, "Computational Electrodynamics: The Finite-Difference Time-Domain Method", Norwood, MA: Artech House, 1995.

[7] S. Grivet-Talocia, "Enforcing Passivity of Macromodels via Spectral Perturbation of Hamiltonian Matrices", *7th IEEE Workshop on Signal Propagation on Interconnects*, May 11-14, 2003, Siena, Italy.

[8] R. Achar, M. Nakhla, "Minimum realization of reduced-order high-speed interconnect macromodels", in *Signal Propagation on Interconnects*, H. Grabinski and P. Nordholz Eds., Kluwer, 1998.

[9] S. Boyd, V. Balakrishnan, P. Kabamba, "A bisection method for computing the H_∞ norm of a transfer matrix and related problems", *Math. Control Signals Systems*, Vol. 2, 1989, pp. 207–219.

[10] S. Grivet-Talocia, I. Maio, I. Stievano, and F. Canavero, "A comparison of reduced-order techniques for complex interconnects modeling," in *2002 IEEE International Symposium on Electromagnetic Compatibility, Minneapolis, Minnesota USA*, pp. 457–462, August 19–23, 2002.